

A quick protocol for the identification and characterization of early growth mutants in tomato

Aurora Alaguero-Cordovilla¹, Francisco Javier Gran-Gómez¹, Paula Jadcza^{1,2}, Mariem Mhimdi¹, Sergio Ibáñez¹, Cécile Bres³, Daniel Just³, Christophe Rothan³, José Manuel Pérez-Pérez^{1,*}

¹ Instituto de Bioingeniería, Universidad Miguel Hernández, 03202 Elche, Alicante, Spain

(A.A.-C., aalaguero@umh.es; M.M., mmhimdi@umh.es; S.I., s.ibanez@umh.es; J.M.P.-P., jmperez@umh.es)

² Present address: Department of Genetics, Plant Breeding and Biotechnology, West Pomeranian University of Technology, 71270 Szczecin, Poland (paula.jadcza@zut.edu.pl)

³ INRAE and University of Bordeaux, UMR 1332 Biologie du Fruit et Pathologie, F-33140, Villenave d'Ornon, France (C.B., cecile.bres@inrae.fr; D.J., daniel.just@inrae.fr; C.R., christophe.rothan@inrae.fr)

Corresponding author: José Manuel Pérez-Pérez (jmperez@umh.es)

Published in:

Alaguero-Cordovilla A, Gran-Gómez FJ, Jadcza P, Mhimdi M, Ibáñez S, Bres C, Just D, Rothan C, Pérez-Pérez JM. A quick protocol for the identification and characterization of early growth mutants in tomato. *Plant Sci.* 2020 Dec;301:110673. doi: 10.1016/j.plantsci.2020.110673. Epub 2020 Sep 14. PMID: 33218638.

Abstract

Root system architecture (RSA) manipulation may improve water and nutrient capture by plants under normal and extreme climate conditions. With the aim of initiating the genetic dissection of RSA in tomato, we established a defined ontology that allowed the curated annotation of the observed phenotypes on 12 traits at four consecutive growth stages. In addition, we established a quick approach for the molecular identification of the mutations associated with the trait-of-interest by using a whole-genome sequencing approach that does not require the building of an additional mapping population. As a proof-of-concept, we screened 4,543 seedlings from 300 tomato M₃ lines (*Solanum lycopersicum* L. cv. Micro-Tom) generated by chemical mutagenesis with ethyl methanesulfonate. We studied the growth and early development of both the root system (primary and lateral roots) and the aerial part of the seedlings as well as the wound-induced adventitious roots emerging from the hypocotyl. We identified 659 individuals (belonging to 203 M₃ lines) whose early seedling and RSA phenotypes differed from those of their reference background. We confirmed the genetic segregation of the mutant phenotypes affecting primary root length, seedling viability and early RSA in 31 M₄ families derived from 15 M₃ lines selected in our screen. Finally, we identified a missense mutation in the *SICESA3* gene causing a seedling-lethal phenotype with short roots. Our results validated the experimental approach used for the identification of tomato mutants during early growth, which will allow the molecular identification of the genes involved.

Keywords

Solanum lycopersicum; Micro-Tom; EMS mutagenesis; root system architecture (RSA); plant phenotyping; whole-genome sequencing

Abbreviations

AR: adventitious root

CESA: cellulose synthase A

emb: *embryo-defective (emb)*

EMS: ethyl methanesulfonate

LR: lateral root

LSD: least significant difference

MT: Micro-Tom

PR: primary root

RSA: root system architecture

SD: standard deviation

SNP: single nucleotide polymorphism

WT: wild type

1. Introduction

In addition to its primary importance as a vegetable crop, cultivated tomato (*Solanum lycopersicum* L.) is used as a model plant for *Solanaceae* genomics (Rothan et al., 2016) and fleshy fruit development (Quinet et al., 2019). Tomato seedlings have poor nitrogen and phosphorus use efficiency and are particularly sensitive to drought; therefore, they require intensive irrigation and fertilization to maintain high yields and fruit quality (Wang and Xing, 2017). Despite the importance of the root system architecture (RSA) in optimal nutrient and water uptake (Kellermeier et al., 2014; Robbins and Dinneny, 2015), our knowledge about the genetic mechanisms that modulate RSA in tomato is limited (Ivanchenko et al., 2015; Toal et al., 2018; Rothan et al., 2019; Cheng et al., 2020). On the other hand, several genes controlling major checkpoints of root development in monocot crops, such as maize (Hochholdinger et al., 2018) and rice (Meng et al., 2019), have been recently characterized from detailed analyses of their mutant phenotypes. The maize mutant *rootless with undetectable meristems1* is defective in lateral root (LR) initiation, and the affected gene encodes a canonical Aux/IAA protein that acts as a transcriptional repressor of downstream targets by interacting with ZmARF25 and ZmARF34 (von Behrens et al., 2011). Furthermore, transcriptome profiling revealed root type-specific transcriptomic reprogramming of pericycle cells in response to local high nitrate stimulation in this species (Yu et al., 2016), which might account for their high developmental RSA plasticity in response to changing soil conditions.

Due to its small size and short life cycle, the Micro-Tom (MT) cultivar was previously proposed as a model for functional genomics in tomato (Emmanuel and Levy, 2002). Since then, a wealth of genetic resources have been developed for this cultivar (Kobayashi et al., 2014; Shikata and Ezura, 2016). Among those, the TOMATOMA mutant database (<https://tomatoma.nbrp.jp/>) contains visible phenotypic data for 10,793 M₂ mutagenized lines generated by ethyl methanesulfonate (EMS) mutagenesis or γ -ray irradiation (Saito et al., 2011; Shikata et al., 2016). The large size of the available MT mutant population increases the chance of isolating allelic variants in selected genes by TILLING (Okabe et al., 2013). Following this approach, several point mutations have been identified in three genes of the L-ascorbic acid biosynthesis pathway, and the corresponding loss-of-function mutants displayed a strong reduction in leaf ascorbate content (Baldet et al., 2013). As with many other tomato cultivars, MT contains

some distinctive mutations: its dwarf and determinate behavior is caused by recessive alleles of the *DWARF* and *SELF-PRUNING* genes, respectively (Martí et al. 2006; Campos et al., 2010). Because these mutations are recessive and the greenhouse-type tomato variety Moneymaker is one of the MT progenitors (Scott and Harbaugh, 1989), the results obtained from MT research can be easily transferred to commercial cultivars by crossing. For example, a weak ethylene receptor allele identified in the MT background line was applied to extend the fruit shelf life of hybrid commercial tomato cultivars (Mubarak et al., 2015). This application supports the potential of MT to become “the mouse model of plant genetics” (Rick, 1991).

The tomato mutant collection used in this work was an EMS mutant population generated in the miniature cultivar MT at INRA Bordeaux (Just et al., 2013; Garcia et al., 2016). The collection comprises ca. 3,500 highly mutagenized mutant families that have been thoroughly phenotyped for approximately 150 plant and fruit traits stored in a web-searchable database. However, this database does not include any information about their root phenotypes (Petit et al., 2014; Musseau et al., 2017). The identification of the causal mutations that underlie particular phenotypes in this collection has been recently facilitated by a whole-genome sequencing-based mapping approach (Garcia et al., 2016). The high mutation frequencies reported in this population (up to 1 mutation per 130 Kb) facilitate saturation mutagenesis; hence, large allelic series for a given gene of interest can be obtained by studying a limited number of mutant lines (Just et al., 2013) (see above). Systematic annotation of mutant phenotypes has been carefully performed in the plant model *Arabidopsis thaliana* by recording the phenotypic descriptions in Plant Ontology and Phenotypic Quality Ontology terms (Akiyama et al., 2014). With the aim of initiating the genetic dissection of root development in tomato, we screened a highly mutagenized MT collection to search for mutants affected in several developmental traits during early growth, focusing on specific RSA phenotypes. We established a controlled vocabulary for the curated annotation of the observed phenotypes. We developed a quick procedure for the molecular identification of causal mutations through a whole-genome sequencing approach. The experimental layout developed here will allow the identification of some of the genetic determinants involved in root development during early growth in tomato through mutant analyses.

2. Materials and methods

2.1. Plant materials and growth conditions

We studied M₃ seeds obtained by selfing 395 M₂ lines (Supplementary Table S1) from a highly mutagenized EMS mutant collection described previously (Just et al., 2013; Petit et al., 2014). For scarification, ~30 seeds per M₃ line were treated with 10% sulfuric acid for 3 min and rinsed thoroughly with sterile water (3 times). Next, seeds were surface-sterilized in 3% (w/v) sodium hypochlorite for 10 min, rinsed with sterile water (4 times), and transferred to wet chambers on a 28°C–dark growth cabinet. Germinated seedlings at 96 h (radicle > 4 mm length) were transferred to 120 mm-square Petri dishes (0 days after sowing) containing 75 mL of sterile half-Murashige and Skoog basal salt medium (Duchefa, The Netherlands), 5 g L⁻¹ plant agar (Duchefa), 0.5 g L⁻¹ 2-(N-morpholino) ethanesulfonic acid (Duchefa) and 2 mL L⁻¹ Gamborg B5 vitamin solution (Duchefa), pH 5.8. Six or seven germinated seedlings were placed on each Petri dish, and three to four dishes per genotype were kept in near-vertical positions in a growth cabinet under 16 h light (average photosynthetic photon flux density of 50 μmol m⁻² s⁻¹) at 26±1°C and 8 h darkness at 23±1°C (Supplementary Figure S1). For the lateral root (LR) capacity assay (Van Norman et al., 2014), 3–4 mm of the root tip was excised after 3 days, and the seedlings were grown for another 5 days (Figure 1A). The formation of adventitious roots (ARs) was then induced by removing the whole root system 2–3 mm above the hypocotyl-root junction with a sharp scalpel after 8 days, and the shoot explants were transferred to sterile 500 mL glass bottles with 75 mL of the plant culture medium.

2.2. Phenotype annotation and microphotography

To describe the observed mutant phenotypes (Figure 1B), we established a controlled vocabulary based on Plant Ontology, Phenotypic Quality Ontology and Environment Ontology terms (Cooper and Jaiswal, 2016; Cooper et al., 2018). We gathered visual information from each seedling for 12 phenotypic traits in several plant structures (i.e., germinated seedlings, primary roots [PR], LRs, shoots and ARs) at four consecutive phenological growth stages (Feller et al., 1995) during the 26 days after seed imbibition (Tables 1 and Supplementary Table S2). LRs and ARs were scored at 8 and 22 days after sowing, respectively (5 and 14 days after LR

and AR induction, respectively). Photographs of the PR, LRs and ARs were taken at the indicated times (Figure 1) using a Sony Cyber-shot DSC-H3 camera (Sony Corporation, Tokyo, Japan) at a resolution of 3,264×2,448 pixels, and the images were saved as RGB color images in the jpeg format.

Chi-square analyses were used to test the goodness-of-fit (p -value<0.05) to expected ratios for the monogenic inheritance of the mutant phenotype in individual M₃ lines (Supplementary Table S3); when two different mutant phenotypes were observed in the same line, we confirmed the independent segregation of the mutant alleles by the chi-square test. Considering a 10% chance of type II error in monogenic inheritance, we did not take into account those lines with fewer than eight WT-like seedlings studied and that did not segregate for the observed mutant phenotypes (Supplementary Table S1).

2.3. Mutant confirmation and whole-genome sequencing

In M₃ lines for which monogenic inheritance for the studied mutations could not be ruled out (Supplementary Table S4), four to six wild-type (WT) siblings were transferred to pots and allowed to self-pollinate in the greenhouse to collect and store M₄ seed families in our seed bank (Figure 1C). Between two and four M₄ families derived from WT-like M₃ plants in the selected lines (16 M₃ lines) were used for segregation studies (Table 2) using the experimental layout described above.

Between 10-24 M₄ WT-like plants from WT-like non-segregating M₃ families and 10-24 M₄ mutant plants from presumably heterozygous-segregating M₃ families were collected to prepare WT-like and mutant bulks, respectively, and were stored at -80°C (Figure 1C). In the case of P14A1, we gathered tissue samples from 20 WT-like and 11 mutant M₄ seedlings from two different M₃ families (P14A1#15 and P14A1#2, respectively). DNA extraction was performed by using the NucleoSpin Plant II commercial kit (Macherey-Nagel Inc. USA) according to the manufacturer's instructions. DNA integrity was evaluated by agarose gel electrophoresis and spectrophotometric methods prior to whole-genome sequencing. Libraries were constructed and sequenced at the Beijing Genomics Institute (BGI, China) using the BGISEQ-500 platform, which is based on novel DNA Nanoball sequencing technology (Zhu et al., 2018). The 150 bp-long paired-end reads that were generated were used for bioinformatics analyses after adapter cleansing and quality checks. To optimize whole-genome coverage, we reconstructed the MT genome sequence file by using the FastaAlternateReferenceMaker tool from the

Genome Analysis Toolkit (McKenna et al., 2010), which implemented polymorphism data from the MT genome into the Heinz 1706-BC reference genome SL3.0 (<https://solgenomics.net/>). Reads were then mapped to this modified reference genome using HISAT2 (Kim et al., 2019), including some parameters that limited the number of polymorphisms per read to a maximum of two. Matrix manipulation was carried out with SAMtools (Li et al., 2009) and Picard Tools (<http://broadinstitute.github.io/picard/>). The polymorphic positions between the WT-like and mutant bulk alignments were extracted with Genome Analysis Toolkit and later filtered to exclusively preserve SNPs. The SNPs mostly consisted of G/C to A/T transitions, as expected for EMS mutations (Shirasawa et al., 2016), with coverage ranging from 10x to 100x. To graphically identify the candidate regions, we used the ratio parameter described elsewhere (Wachsman et al., 2017), which consists of the difference between the reference allelic frequency in the WT-like bulk and the reference allelic frequency in the mutant bulk. Graphic representation smoothing was achieved by applying the moving average method with a window width of five genomic coordinates (Beissinger et al., 2015).

We confirmed the presence of single nucleotide polymorphism (SNP) candidate n^o7 in ten WT-like seedlings derived from P14A1 #15 and P14A1 #2, as well as in 5 seedling-lethal plantlets derived from P14A1 #2, by using the primer pairs SICESA3-F (TACTGTATGCCCAAGAGACCC) and SICESA3-R (ACTTGACTTTTGGAACTTGTGG) for PCR amplification, followed by PCR product purification and Sanger sequencing using the SICESA3-F primer. The presence of the SNP candidate n^o3 was also evaluated in the same seedlings by using the primer pairs Solyc01g073770-F (ACCCAATTCAGATTAC) and Solyc01g073770-R (CTCTTCCTTCGCTACATCAGC). Solyc01g073770-F was used for Sanger sequencing. The 3D structure analysis of the CESA protein was carried out with the program PyMOL (DeLano Scientific LLC, 2006) available at <http://www.pymol.org>.

2.4. Chemical inhibition of cellulose biosynthesis

MT seedlings were sterilized as described in section 2.1 and placed in 90 mm-diameter Petri dishes containing 40 mL sterile plant culture medium supplemented with 0 nM (mock), 10 nM or 40 nM isoxaben (Merck, USA) and incubated in a 28°C-dark growth cabinet for three days. Then, half of the Petri dishes were transferred to standard growing conditions, while the other half ones remained in darkness. After three days, photographs were

taken using the Sony Cyber-shot DSC-H3 camera (Sony Corporation, Tokyo, Japan). PR length was measured and analyzed from the image files with ImageJ (Schneider et al., 2012).

2.5. Statistical analysis

Descriptive statistics (average, standard deviation [SD], median, etc.) were calculated using GraphPad Prism version 8.3.1 for Windows (GraphPad Software, La Jolla California USA). Data outliers were identified based on aberrant SD values and excluded for posterior analyses (Aguinis et al., 2013). Average values \pm SDs are shown in the graphs, except in cases that did not exhibit a normal distribution and for which the median was used instead. We performed multiple testing analyses using the Fisher's least significant difference (LSD) method (p -value <0.01). Nonparametric tests were used when necessary.

3. Results

3.1. Early seedling and root architecture mutant phenotype screening

Following the scheme shown in Figure 1, we searched for mutant phenotypes during early growth in 9,367 M_3 seedlings derived from 395 M_3 lines. Overall, we found lower germination rates in the studied M_3 lines ($53.4\pm 21.5\%$) than in the MT background line ($87.9\pm 15.2\%$; Supplementary Figure S2). We discarded 95 M_3 lines (24.1% of M_3 lines; indicated in bold in Supplementary Table S1) whose low germination rates led to a reduced number of seedlings ($n<8$), which made the identification of recessive mutant seedlings difficult. Therefore, we studied the early seedling and rooting phenotypes in 4,543 seedlings from 300 M_3 lines. We manually annotated the phenotypic differences in the early RSA and seedling growth of the MT background line in 946 seedlings from 252 M_3 lines (20.8% of the studied seedlings and 84.0% of the studied M_3 lines; Supplementary Tables S2 and S3).

3.2. Mutants defective in embryo development and early shoot growth

We found 235 seedlings with seedling-lethal phenotypes (5.2% of studied seedlings and 24.8% of annotated mutants) that were similar to the *embryo-defective* (*emb*) mutants of *Arabidopsis thaliana* (Meinke, 2019). The observed seedling-lethal phenotypes segregated as a recessive trait in 87 of the studied M₃ lines (29.0%; Tables S3 and S4). These results are in agreement with the high mutation rates previously reported in this population (Garcia et al., 2016). Only in P11H6 was the phenotypic segregation of the observed seedling-lethal phenotype likely due to a dominant effect of the causal mutation. Twenty-one of these lines segregated as seedlings that were unable to elongate the radicle and stopped growing at stage 005 (shown as [0] on Supplementary Tables S3 and S4). The other seedlings survived through stage 005 but showed striking alterations in the development of their apical-basal axis and were named Emb-1 to Emb-4 (shown as [1] to [4] on Supplementary Tables S3 and S4) depending on the missing developmental structure (Figure 2A). We found 25 lines segregating for putative recessive mutations that caused the Emb-1 phenotype, which is characterized by the absence/disruption of the apical region of the embryo (i.e., the cotyledons and the shoot apical meristem; Figures 2A, 2B); these resembled the *gurke* mutants of *Arabidopsis* (Mayer et al., 1991). Four and three lines were in turn found to segregate for Emb-2 and Emb-4 phenotypes (Figures 2A, 2B and Supplementary Table S3), which were reminiscent of the *monopteros* and *gnom* mutants, respectively (Mayer et al., 1991). Interestingly, we found 34 M₃ lines that segregated for more than one Emb-like phenotype within the same line (Figure 2C), indicating a complex disturbance of embryo development in these lines. However, these results are a clear underestimation of all the seedling-lethal phenotypes segregating in the MT EMS-mutagenized population; many seeds were unable to germinate (Supplementary Figure S2), and we did not study their embryo phenotypes in detail.

We found 91 seedlings from 49 M₃ lines (2.0% of studied seedlings and 9.6% of annotated mutants) with some variation in their shoot phenotype compared to that of the MT background line (Supplementary Table S4). We clearly distinguished between seedlings with “delayed growth” or “dwarf” phenotypes, the latter being characterized by reduced size in all tissues compared with those of their WT siblings. Thirty-three seedlings from 13 M₃ lines were defined as “dwarf” and likely contain recessive mutations that mostly affect cell growth (Figure 3D and Supplementary Table S4), as eight of these lines also caused PR growth defects in the same plants (see next

section). On the other hand, 22 seedlings from 11 M₃ lines annotated as “delayed shoot growth” did not affect root growth. Three other lines, P12A2, P14C10 and P15H6, segregated for albino plants. Additionally, we found that seven out of 20 M₃ lines segregated for individuals with three cotyledons, but no other phenotypic RSA alterations were observed in these seedlings (Supplementary Tables S3 and S4).

3.3. Early seedling root growth mutants

PR morphologies were studied at 3 days, and the mutant phenotypes found were visually assigned to six categories according to PR length, root hair distribution, or root gravitropism alterations. We found 465 seedlings in 160 M₃ lines with some alteration in PR morphology, most of which displayed shorter PRs or with a premature differentiation of the PR (427 seedlings and 145 M₃ lines; 9.4% of studied seedlings and 45.1% of annotated mutant seedlings; Figure 3A and Supplementary Table S3). Only in three of the lines (P11H11, P12A12 and P15A1) did the short-root phenotype segregate as a dominant trait, while the phenotype of the P11G10 line was likely fixed from the previous generation (Supplementary Tables S3 and S4). Ten lines were characterized by the presence of several seedlings with significantly (p -value <0.01) longer PRs (57.9 ± 15.1 mm; $n=25$ seedlings) than their WT-like siblings (27.7 ± 12.4 mm; $n=100$ seedlings; Figure 3A). We identified five seedlings in two M₃ lines, P15G2 and P16A11, and four in the P15A6 line, with higher and lower root hair densities, respectively (Figure 3B and Supplementary Table S3). We found six seedlings in three M₃ lines (P11G11, P12A4 and P13D11) with agravitropic root responses, as their PR growth was not oriented towards the gravity vector (Figure 3C). In all these lines, the agravitropic mutant phenotypes were likely caused by recessive mutations (Supplementary Table S4).

We studied LR architecture at 5 days after surgical excision of the PR tip (see Materials and Methods), which induced the emergence of LR primordia derived from already-specified LR founder cells (Moreno-Risueno et al., 2010; Du and Scheres, 2018). We found 141 seedlings in 43 M₃ lines with altered LR numbers (3.1% of studied seedlings and 14.9% of annotated mutants). Thirty-two lines displayed segregation for a decreased amount of LRs (3.4 ± 1.8 ; $n=73$ seedlings) compared with their WT siblings (12.4 ± 5.4 ; $n=376$ seedlings), which were likely caused by recessive mutations (Figure 3D and Supplementary Table S3). Thirty-six seedlings from 12 lines were unable to produce any LRs after root tip excision,

suggesting that their causal mutations might affect the positive regulators of LR formation. On the other hand, 34 seedlings from 11 M₃ lines displayed an increased number of LRs (35.4 ± 7.3) compared to their WT-like siblings (p -value <0.01 ; Figure 3D and Supplementary Table S3), and their mutations might affect negative regulators of LR growth.

Sixteen of the studied M₃ lines were annotated to segregate for seedling phenotypes affecting several PR and LR attributes (Supplementary Table S4). In 11 of them, different seedlings displayed either PR length or LR number mutant phenotypes, suggesting that different mutations independently affected those two phenotypic traits. The other three lines contained seedlings with pleiotropic phenotypes regarding PR length and LR number. On the one hand, the segregating mutations in P13C12 and P15A4 reduced both PR length and LR number, whereas the segregating mutation in P16E10 reduced PR length, but the number of LRs increased (Supplementary Table S4).

3.4. Mutants affected in wound-induced AR formation

ARs arising from the hypocotyl were studied after the removal of the whole root system at 8 days (see Materials and Methods). We identified 105 seedlings from 48 M₃ lines with some alterations in wound-induced AR formation (2.3% of studied seedlings and 11.1% of annotated mutants; Figure 4A and Supplementary Table S3) in proportions that were consistent with recessive inheritance of the mutant phenotypes in most cases (47 M₃ lines; Supplementary Table S4). Thirty-six M₃ lines included some seedlings with a significant reduction in AR number (1.6 ± 1.3 ; $n=35$ seedlings in 13 M₃ lines) compared with their WT-like siblings (6.9 ± 3.0 ; $n=135$ seedlings; Figure 4B) or did not produce any AR under our experimental conditions ($n=46$ seedlings in 23 M₃ lines). Twenty-four individuals from 11 M₃ lines displayed a significant increase in AR number (14.3 ± 5.6 ; Figure 4B) compared to their WT-like siblings (5.7 ± 3.0 ; $n=127$ seedlings; p -value <0.001).

We found a substantial overlap (64.5%) in the M₃ lines of seedlings with wound-induced AR mutant phenotypes and those with PR and LR mutant phenotypes (Figure 4C). However, most of these lines segregated for the observed mutant phenotypes in different seedlings, suggesting that different mutations altered the PR, LR and AR traits independently (Supplementary Table S4). Only in P13D11 and P14C12 did we find several seedlings displaying reductions in both PR length and wound-induced ARs (Supplementary Table S4). Intriguingly, the mutation present

in P13D11 also altered PR gravitropism. Our results suggested that the causal mutations in these lines would affect the shared pathways required for postembryonic root development. On the other hand, we found 17 M₃ lines segregating for seedlings with altered numbers of wound-induced ARs with no pleiotropic effects on other RSA traits (Figure 4C and Supplementary Table S4). Among these, segregating mutations in P12F10, P14F11, P14G10, P15G12 and P16H11 caused an increased number of ARs only and might have affected some of the negative regulators required for the early stages of wound-induced AR formation; these mutations deserve further investigation.

3.5. Confirmation of tomato mutants affected in early growth

We estimated the number of mutations and their inheritance patterns in the studied M₃ lines that affected early seedling and RSA traits (Supplementary Table S4). The number of mutations found resembled a Poisson distribution with $\lambda=1.65$ (Figure 4D). To confirm the genetic basis of the observed mutant phenotypes, we selected 14 M₃ seed batches that segregated for mutants with shorter PRs and one that segregated for longer PRs. We studied the phenotypic segregation for the annotated mutants in 27 M₄ families obtained by selfing several M₃ plants that displayed a WT-like phenotype from each of these lines (71.0%; Supplementary Table S5). We assessed the recessive inheritance of the shorter PR phenotype in 11 of the 18 M₄ families (61.1%) derived from P11H8, P12A1, P12A6, P12C12, P12D2 and P12G2 (Table 2 and Figure 5A).

In addition, we found that the P11H4, P14A1, P14A9, P14A12, P14B4 and P14C12 lines segregated for two independent mutations, one affecting PR length and the other affecting seedling lethality; that all three M₄ families from P16F4 segregated for seedlings with longer PRs; and that two families in this line segregated for a seedling-lethal phenotype (Table 2). The results found in P11H4, P14A1, P14B4, P14C12 and P16F4 are in agreement with the hypothesis that the two mutations segregate independently, as they might be located on different chromosomes. However, we were not able to confirm the genetic basis of the shorter PR phenotype from P12A7 due to the lack of mutants in the three M₄ families derived from this line (Table 2 and Supplementary Table S5).

We studied five other M₄ families derived from P14D10 and P14D2, segregating in the M₃ for seedlings with a decreased number of LRs or ARs, respectively. We found nine seedlings with a significantly reduced number

of ARs (1.5 ± 0.9) in two M_4 P14D2 families as compared with those of their WT siblings (4.8 ± 1.3 ; $n=52$; $p\text{-value}<0.01$; Table 2 and Figure 5B).

3.6. Molecular identification of a gene required for embryo development and early root growth

In our phenotypic screen, we found a significant number of seedlings from M_3 seed batches that displayed seedling-lethal phenotypes. We further confirmed in M_4 the recessive inheritance of some of these seedling-lethal phenotypes in four lines derived from P14 (A1, A9, B4, and C12), P11H4 and P16F4 (Table 2 and Supplementary Table S5). In the studied lines, the seedling-lethal phenotypes segregated in a proportion compatible with single recessive mutations in eight of the M_4 families studied (40.0%, Table 2). The M_3 mutants segregating in P14A1 exhibited a characteristic seedling-lethal phenotype of defective (or very short) PR growth, cotyledon expansion defects and the absence (or severe delay) of the shoot apex (Figure 6A). SNP calling between mutant and WT genomic sequences allowed us to identify (and to discard) non-causal mutations in the genetic background of the P14A1 line, as well as several SNPs between mutant and WT-like bulks (Supplementary Table S6). We focused on 24 SNPs (G/C to A/T transitions) located in the long arm of chromosome 1 (Figure 6B) with ratio values ~ 1 , indicating high mutant allelic frequencies in the mutant bulk ($n=11$ mutant seedlings), while the ratio values in the WT-like bulk ($n=20$ WT-like seedlings derived from non-segregating M_3 families for the studied mutant phenotype ; see Materials and Methods) were close to zero. SNP candidate n°3 (Supplementary Table S6) is responsible for an arginine-to-glutamic acid mutation at the 27th residue of Solyc01g073770, a protein similar to At5g19900, whose function is unknown. Another of the studied SNPs (candidate n°7) affected the coding region of the cellulose synthase A (CESA) catalytic subunit encoded by Solyc01g087210 (Figure 6B and Supplementary Table S6). To identify the causal mutation, we sequenced the region including these SNPs in several WT-like and mutant seedlings from the #2 and #15 M_4 families (see Materials and Methods). Plants displaying the mutant phenotype were homozygous for the mutated allele containing the SNP candidate n°7 in homozygosity (Figure 6C), while segregated for the SNP candidate n° 3. Based on the PROVEAN analysis tool (http://provean.jcvi.org/seq_submit.php), the Arg-toGlu²⁷ mutation was considered neutral for the Solyc01g073770 protein, while the Leu-to-Phe⁸⁶⁹ mutation in the CESA protein was deleterious. These results suggest that the missense mutation in Solyc01g087210, which causes a leucine-to-

phenylalanine substitution at the conserved position 869 of the fifth transmembrane domain of the CESA protein (Figure 6D), might affect the stability of the transmembrane domain of the protein (Figure 6E) and therefore its function.

To further analyze the consequences of cellulose synthase inactivation on early growth of tomato seedlings, we studied the effect of the chemical inhibition of its activity by isoxaben, a well-known inhibitor of cellulose synthesis that interferes with the correct insertion of cellulose synthase A into the plasma membrane (Tateno et al., 2016). Germinated MT seedlings in the presence of isoxaben (both 10 and 40 nM) resembled the seedling-lethal phenotype observed in the P14A1 M₃ and M₄ lines studied (Figure 6F). PR growth was severely impaired in the isoxaben-treated MT seedlings, even at the lowest concentration used, causing a >80% PR length reduction when compared to that in the non-treated MT seedlings (Figure 6G). Taken together, our results suggest that the missense mutation found in Solyc01g087210 disrupts SICES3A activity and may be responsible for the observed seedling-lethal phenotype in P14A1.

4. Discussion

A systematic observation of mutant phenotypes caused by loss-of-function alleles is required to elucidate gene function through forward genetic analysis. In *Arabidopsis thaliana* (Arabidopsis), several large-scale phenotypic analyses have generated huge phenotypic data sets, most of which are publicly available (Ajjawi et al., 2010; Lloyd and Meinke, 2012; Myouga et al., 2013; Akiyama et al., 2014; Wilson-Sánchez et al., 2014; Meinke, 2019). Tomato (*Solanum lycopersicum* L.) was proposed as an alternative model for the study of particular traits not found in Arabidopsis, such as fleshy fruit and compound leaf development (Rothan et al., 2016). However, reliable comparative studies of mutations affecting genes in the same pathway are lacking in this species due to large differences in the genetic backgrounds of the different cultivars studied (Carvalho et al., 2011). In an attempt to initiate the genetic dissection of RSA in tomato, we developed an appropriate experimental framework for the identification of tomato mutants affected in 12 phenotypic traits at four consecutive phenological growth stages. Forward genetic approaches provide access to species-specific gene functions, which will contribute to the better understanding of the studied traits. In this work, a subset (n=300 M₃ lines) of a highly chemically mutagenized mutant collection in the miniature

determinate cultivar MT was screened for early seedling and root mutant phenotypes (20 traits). We observed that 37% of the studied M₃ lines segregated for several mutant traits in different plants, such as seedling lethality or PR growth, which is indicative of the large number of homozygous mutations present in the EMS-mutagenized collection studied (Garcia et al., 2016).

To facilitate the subsequent identification of the causal mutation through whole-genome sequencing, we developed a procedure of preparing the mutant bulks by combining the mutant seedlings collected from the segregating M₄ families and preparing the WT bulks by combining the WT-like seedlings collected from the non-segregating M₄ families. As a proof-of-concept, we identified the mutation associated with the seedling-lethal phenotype of the P14A1 line. Mutants defective in embryo development were commonly found in mutagenized Arabidopsis collections, with the frequency of mutant seeds in heterozygous siliques ranging from 5% to 50% (Meinke, 2019). To date, more than 2,200 mutants affecting 510 *EMB* genes (1.8% of all coding genes) have been identified in Arabidopsis, most of which encode chloroplast-localized proteins, proteins involved in RNA binding and modification, or multiple components of essential protein complexes (Meinke, 2019). Following a method for bulk sequencing previously used in rice (Fekih et al., 2013) that does not require the building of a new mapping population, we were able to identify a missense mutation in the coding region of Solyc01g087210 in the seedling-lethal mutants of the P14A1 line. This mutation changed a conserved leucine-to-phenylalanine residue in the fifth transmembrane domain of the protein, which might affect its stability. Solyc01g087210 encodes the catalytic subunit of cellulose synthase A, CESA3, which forms a large plasma membrane-localized cellulose-synthesizing complex with CESA1 and CESA6 required for primary cell wall biosynthesis in Arabidopsis (Carroll et al., 2012). Null mutations of *CESA1* in Arabidopsis, also named *RADIALLY SWOLLEN1*, produce extreme defects in the primary cell wall and cell shape, which lead to a seedling-lethal phenotype (Beeckman et al., 2002) that is indistinguishable from the tomato seedling-lethal mutant found in P14A1 (this work). The Arabidopsis CESA3 is coexpressed with CESA1, and null *cesa3* alleles are lethal to male gametophytes (Persson et al., 2007). Interestingly, a missense semidominant mutation affecting the conserved proline-578 residue of CESA3 in Arabidopsis also caused a characteristic seedling-lethal phenotype (Daras et al., 2009) that is indistinguishable from that described above in P14A1. In addition, a forward genetic screen in Arabidopsis identified a missense mutation in the sixth transmembrane

domain of CESA1 (Ala-to-Val⁹⁰³) that increased cellulose synthase movement in the plasma membrane and produced structurally aberrant cellulose microfibrils (Harris et al., 2012). We were able to mimic the seedling-lethal phenotype of P14A1 by incubating WT tomato seeds on isoxaben, a known inhibitor of the cellulose synthase activity (Burn et al., 2002; Pysh et al., 2012). Taken together, we propose that the missense mutation identified in P14A1 (Leu-to-Phe⁸⁶⁹) affects the activity of the cellulose-synthesizing complex in tomato, which is essential for primary cell wall biosynthesis.

The most frequent mutant phenotypes found in our phenotypic screen affected PR growth, with a high prevalence of seedlings with shorter roots than the WT (in 47.0% of the studied lines). PR growth depends on the production of new cells in the meristem and their subsequent expansion in the elongation zone of the root (Petricka et al., 2012). In Arabidopsis, many recessive mutations result in shorter root lengths than in the WT. On the one hand, mutations in the brassinosteroid pathway led to a significant reduction in shoot as well as root size and are considered dwarf mutants (Fridman and Savaldi-Goldstein, 2013). On the other hand, mutations in the gibberellin pathway mostly affected shoot growth (and as such are considered semidwarfs) and might confer a selective advantage under specific environmental conditions, such as drought (Barboza-Barquero et al., 2015). We found seedlings with dwarf (shoot and root) phenotypes segregating as a single recessive trait in 13 M₃ lines; in six of these lines, other seedlings displayed decreased PR lengths, suggesting that additional mutations specifically affecting PR growth could also be segregating. We found three lines where the short-root phenotype segregated as a dominant trait; these seedlings also displayed a characteristic pleiotropic phenotype consisting of a twisted hypocotyl and delayed shoot growth. Because the number of dominant mutations with a short-root phenotype in Arabidopsis is limited (Meinke, 2013) and most of them directly affect the auxin pathway (i.e., *YUCCA*, *SHORT HYPOCOTYL2* and *CRANE*), a candidate gene approach will facilitate the identification of causal mutations in these tomato lines. We are conducting allelism tests between some of the short-root tomato mutants that we identified to initiate the bulk of allelic mutant seedlings required for the whole-genome sequencing approach described here.

We found seedlings with agravitropic root and/or shoot growth in four M₃ lines (P11G11, P12A4, P12H3 and P16H8). We will confirm the recessive inheritance of this phenotype in M₄ families, while crosses among the agravitropic mutants from different lines will allow us to determine the number of genes affected in these mutants. Several genetic loci have been

identified as being involved in root gravitropism in *Arabidopsis* (Su et al., 2017), a process that is directly dependent on the intracellular auxin gradient in the elongation zone of the root established by dynamic PIN-FORMED polarity establishment at the cell membrane (Abas et al., 2006; Rosquete et al., 2013). The *diageotropica* tomato mutant, affected by polar auxin efflux within the root, displays reduced gravitropic responses (Oh et al., 2006; Ivanchenko et al., 2015). On the other hand, in the *polycotyledon* mutant, with enhanced polar auxin transport, a higher root gravitropic curvature was observed compared with that in the WT (Al-Hammadi et al., 2003). Whole-genome sequencing will allow us to identify the genes altered in the agravitropic tomato mutants found in our screen.

Interestingly, we found seedlings with significantly longer PR lengths segregating in a recessive manner in ten M₃ lines; their mutations might affect the negative regulators of root growth. A number of recessive mutants in *Arabidopsis* with longer roots revealed an interesting crosstalk between jasmonic acid and auxin (Khan and Stone, 2007; Zheng et al., 2016). As deeper roots may be advantageous for water capture from the subsoil in dry environments, increasing our knowledge of the molecular pathways involved in such processes in tomato is of utmost importance for increasing yield in adverse environments.

Both LRs and ARs are essential for increasing the surface area of root systems to explore heterogeneous soil environments in different species (Atkinson et al., 2014; Banda et al., 2019). *De novo* root formation can be divided into several developmental stages, and a number of different mutants have been identified as being affected in specific LR stages (Banda et al., 2019). We found 11 M₃ tomato lines with a significant increase in LR number. The *anthocyanin-reduced* tomato mutant, which is defective in the gene encoding FLAVONOID 3-HYDROXYLASE, the first step in flavonol synthesis, developed 50% fewer LRs than the wild type (Maloney et al., 2014). Conversely, the *anthocyanin without* tomato mutant, with increased flavonol levels, displayed a significant increase in the number of LRs compared with the WT (Maloney et al., 2014). Additional experiments suggested that flavonols reduce auxin flux through WT roots, enhancing the accumulation of auxin at sites of LR formation (Maloney et al., 2014). A time-series analysis of LR formation, as well as a study of the effect of exogenously applied auxin and/or flavonols, in the MT mutants identified here will help us to define the developmental pathway affected in these mutants and would surely help with candidate gene assignment after whole-genome sequencing.

5. Conclusions

We aimed to develop a standardized experimental procedure for root trait screening in young tomato seedlings using a thoroughly characterized EMS-mutagenized collection on the MT background (Just et al., 2013). We were able to identify and confirm a number of recessive mutations that affect several RSA traits, such as PR length, LR number and AR initiation. We established a whole-genome sequencing approach by using WT-like and mutant bulks from non-segregating and segregating M_3 families that allowed us to identify a missense mutation in *SICESA3* that was associated with a seedling-lethal phenotype with very short roots. Further work will allow us and others to identify some of the key molecular players involved in RSA in tomato, which will help us to increase our understanding of RSA plasticity in response to environmental conditions.

Author contributions

Conceptualization, J.M.P.-P.; methodology, A.A.-C., F.G.-G., P.J. and J.M.P.-P.; investigation, A.A.-C., F.G.-G., P.J., M.M., C.B. and S.I.; resources, D.J., C.B. and C.R.; data curation, A.A.-C. and J.M.P.-P.; writing—original draft preparation, A.A.-C. and J.M.P.-P.; writing—review and editing, C.R. and J.M.P.-P.; supervision, J.M.P.-P.; project administration, J.M.P.-P.; funding acquisition, J.M.P.-P. All authors have read and agreed to the published version of the manuscript.

Declaration of Competing Interest

The authors declare that there are no conflicts of interest.

Acknowledgements

We thank María José Níguez for her expert technical assistance and David Esteve-Bruna for help during the setup of the whole-genome sequencing approach.

Funding

This research was funded by the Ministerio de Ciencia e Investigación of Spain (grant numbers BIO2015-64255-R and RTI2018-096505-B-I00) the Conselleria d'Educació, Cultura i Sport of the Generalitat Valenciana (grant numbers IDIFEDER/2018/016 and PROMETEO/2019/117), and the European Regional Development Fund of the European Commission. SI and MM are research fellows of the Generalitat Valenciana (grant numbers ACIF/2018/220 and GRISOLIAP/2019/098).

Appendix. Supplementary data

The following is Supplementary data to this article:

Supplementary Figure S1. Air temperature and relative humidity during the phenotype screening

Supplementary Figure S2. Germination percentage for the studied lines

Supplementary Table S1. Tomato EMS lines studied

Supplementary Table S2. Ontology annotations

Supplementary Table S3. Individual data values of the studied M₃ lines

Supplementary Table S4. Segregation studies of the studied M₃ lines

Supplementary Table S5. Individual data values of the studied M₄ lines

Supplementary Table S6. Candidate SNPs of P14A1 in chromosome 1

References

- Abas L, Benjamins R, Malenica N, Paciorek TT, Wiřniewska J, Moulinier-Anzola JC, Sieberer T, Friml J, Luschnig C** (2006) Intracellular trafficking and proteolysis of the Arabidopsis auxin-efflux facilitator PIN2 are involved in root gravitropism. *Nat Cell Biol* **8**: 249–256
- Aguinis H, Gottfredson RK, Joo H** (2013) Best-Practice Recommendations for Defining, Identifying, and Handling Outliers. *Organ Res Methods* **16**: 270–301
- Ajjawi I, Lu Y, Savage LJ, Bell SM, Last RL** (2010) Large-scale reverse genetics in Arabidopsis: Case studies from the Chloroplast 2010 project. *Plant Physiol* **152**: 529–540

- Akiyama K, Kurotani A, Iida K, Kuromori T, Shinozaki K, Sakurai T** (2014) RARGE II: An Integrated Phenotype Database of Arabidopsis Mutant Traits Using a Controlled Vocabulary. *Plant Cell Physiol* **55**: e4–e4
- Al-Hammadi ASA, Sreelakshmi Y, Negi S, Siddiqi I, Sharma R** (2003) The polycotyledon mutant of tomato shows enhanced polar auxin transport. *Plant Physiol* **133**: 113–125
- Atkinson JA, Rasmussen A, Traini R, Voß U, Sturrock C, Mooney SJ, Wells DM, Bennett MJ** (2014) Branching out in roots: uncovering form, function, and regulation. *Plant Physiol* **166**: 538–50
- Baldet P, Bres C, Okabe Y, Mauxion J-P, Just D, Bournonville C, Ferrand C, Mori K, Ezura H, Rothan C** (2013) Investigating the role of vitamin C in tomato through TILLING identification of ascorbate-deficient tomato mutants. *Plant Biotechnol* **30**: 309–314
- Banda J, Bellande K, von Wangenheim D, Goh T, Guyomarc'h S, Laplaze L, Bennett MJ** (2019) Lateral Root Formation in Arabidopsis: A Well-Ordered LRExit. *Trends Plant Sci* **24**: 826–839
- Barboza-Barquero L, Nagel KA, Jansen M, Klasen JR, Kastenholz B, Braun S, Bleise B, Brehm T, Koornneef M, Fiorani F** (2015) Phenotype of *Arabidopsis thaliana* semi-dwarfs with deep roots and high growth rates under water-limiting conditions is independent of the *GA5* loss-of-function alleles. *Ann Bot* **116**: 321–331
- Beeckman T, Przemeck GKH, Stamatiou G, Lau R, Terryn N, De Rycke R, Inzé D, Berleth T** (2002) Genetic complexity of cellulose synthase A gene function in arabidopsis embryogenesis. *Plant Physiol* **130**: 1883–1893
- von Behrens I, Komatsu M, Zhang Y, Berendzen KW, Niu X, Sakai H, Taramino G, Hochholdinger F** (2011) Rootless with undetectable meristem 1 encodes a monocot-specific AUX/IAA protein that controls embryonic seminal and post-embryonic lateral root initiation in maize. *Plant J* **66**: 341–353
- Beissinger TM, Rosa GJ, Kaeppler SM, Gianola D, De Leon N** (2015) Defining window-boundaries for genomic analyses using smoothing spline techniques. *Genet Sel Evol*. doi: 10.1186/s12711-015-0105-9
- Burn JE, Hocart CH, Birch RJ, Cork AC, Williamson RE** (2002) Functional analysis of the cellulose synthase genes *CesA1*, *CesA2*, and *CesA3* in Arabidopsis. *Plant Physiol* **129**: 797–807

- Campos ML, Carvalho RF, Benedito VA, Peres LEP** (2010) The micro-tom model system as a tool to discover novel hormonal functions and interactions. *Plant Signal Behav* **5**: 267–270
- Carroll A, Mansoori N, Li S, Lei L, Vernhettes S, Visser RGF, Somerville C, Gu Y, Trindade LM** (2012) Complexes with mixed primary and secondary cellulose synthases are functional in Arabidopsis plants. *Plant Physiol* **160**: 726–737
- Carvalho RF, Campos ML, Pino LE, Crestana SL, Zsögön A, Lima JE, Benedito VA, Peres LE** (2011) Convergence of developmental mutants into a single tomato model system: “Micro-Tom” as an effective toolkit for plant development research. *Plant Methods* **7**: 18
- Cheng W, Yin S, Tu Y, Mei H, Wang Y, Yang Y** (2020) SICAND1, encoding cullin-associated Nedd8-dissociated protein 1, regulates plant height, flowering time, seed germination, and root architecture in tomato. *Plant Mol Biol*. doi: 10.1007/s11103-020-00963-7
- Cooper L, Jaiswal P** (2016) The plant ontology: A tool for plant genomics. *Methods Mol. Biol.* Humana Press Inc., pp 89–114
- Cooper L, Meier A, Laporte M-A, Elser JL, Mungall C, Sinn BT, Cavaliere D, Carbon S, Dunn NA, Smith B, et al** (2018) The Planteome database: an integrated resource for reference ontologies, plant genomics and phenomics. *Nucleic Acids Res* **46**: D1168–D1180
- Daras G, Rigas S, Penning B, Milioni D, McCann MC, Carpita NC, Fasseas C, Hatzopoulos P** (2009) The thanatos mutation in Arabidopsis thaliana cellulose synthase 3 (AtCesA3) has a dominant-negative effect on cellulose synthesis and plant growth. *New Phytol* **184**: 114–126
- Du Y, Scheres B** (2018) Lateral root formation and the multiple roles of auxin. *J Exp Bot* **69**: 155–167
- Emmanuel E, Levy AA** (2002) Tomato mutants as tools for functional genomics. *Curr Opin Plant Biol* **5**: 112–117
- Fekih R, Takagi H, Tamiru M, Abe A, Natsume S, Yaegashi H, Sharma S, Sharma S, Kanzaki H, Matsumura H, et al** (2013) MutMap+: Genetic Mapping and Mutant Identification without Crossing in Rice. *PLoS One* **8**: e68529
- Feller C, Bleiholder H, Buhr L, Hack H, Hess M, Klose R, Meier U, Stauss R, Van den Boom T, Weber E** (1995) Phänologische entwicklungsstadien von

gemüsepflanzen: II. Fruchtgemüse und hülsenfrüchte. Nachrichtenbl Deut Pflanzenschutzd **47**: 217–232

Fridman Y, Savaldi-Goldstein S (2013) Brassinosteroids in growth control: How, when and where. *Plant Sci* **209**: 24–31

Garcia V, Bres C, Just D, Fernandez L, Tai FWJ, Mauxion JP, Le Paslier MC, Bérard A, Brunel D, Aoki K, et al (2016) Rapid identification of causal mutations in tomato EMS populations via mapping-by-sequencing. *Nat Protoc* **11**: 2401–2418

Harris DM, Corbin K, Wang T, Gutierrez R, Bertolo AL, Petti C, Smilgies DM, Estevez JM, Bonetta D, Urbanowicz BR, et al (2012) Cellulose microfibril crystallinity is reduced by mutating C-terminal transmembrane region residues CESA1 A903V and CESA3 T942I of cellulose synthase. *Proc Natl Acad Sci U S A* **109**: 4098–4103

Hochholdinger F, Yu P, Marcon C (2018) Genetic Control of Root System Development in Maize. *Trends Plant Sci* **23**: 79–88

Ivanchenko MG, Zhu J, Wang B, Medvecká E, Du Y, Azzarello E, Mancuso S, Megraw M, Filichkin S, Dubrovsky JG, et al (2015) The cyclophilin a DIAGEOTROPICA gene affects auxin transport in both root and shoot to control lateral root formation. *Dev* **142**: 712–721

Just D, Garcia V, Fernandez L, Bres C, Mauxion J-P, Petit J, Jorly J, Assali J, C[^]acute, Bournonville L, et al (2013) Micro-Tom mutants for functional analysis of target genes and discovery of new alleles in tomato. *Plant Biotechnol* **30**: 225–231

Kellermeier F, Armengaud P, Seditas TJ, Danku J, Salt DE, Amtmann A (2014) Analysis of the root system architecture of *Arabidopsis* provides a quantitative readout of crosstalk between nutritional signals. *Plant Cell* **26**: 1480–1496

Khan S, Stone J (2007) *Arabidopsis thaliana* GH3.9 in Auxin and Jasmonate Cross Talk. *Plant Signal Behav* **2**: 483–485

Kim D, Paggi JM, Park C, Bennett C, Salzberg SL (2019) Graph-based genome alignment and genotyping with HISAT2 and HISAT-genotype. *Nat Biotechnol* **37**: 907–915

Kobayashi M, Nagasaki H, Garcia V, Just D, Bres C, Mauxion JP, Le Paslier MC, Brunel D, Suda K, Minakuchi Y, et al (2014) Genome-wide analysis of intraspecific dna polymorphism in “micro-tom”, a model cultivar of

- tomato (*solanum lycopersicum*). *Plant Cell Physiol* **55**: 445–454
- Li H, Handsaker B, Wysoker A, Fennell T, Ruan J, Homer N, Marth G, Abecasis G, Durbin R** (2009) The Sequence Alignment/Map format and SAMtools. *Bioinformatics* **25**: 2078–2079
- Lloyd J, Meinke D** (2012) A comprehensive dataset of genes with a loss-of-function mutant phenotype in *Arabidopsis*. *Plant Physiol* **158**: 1115–1129
- Maloney GS, DiNapoli KT, Muday GK** (2014) The anthocyanin reduced tomato mutant demonstrates the role of flavonols in tomato lateral root and root hair development. *Plant Physiol* **166**: 614–31
- Martí E, Gisbert C, Bishop GJ, Dixon MS, García-Martínez JL** Genetic and physiological characterization of tomato cv. Micro-Tom. doi: 10.1093/jxb/erj154
- Mayer U, Ruiz RAT, Berleth T, Miseéra S, Jürgens G** (1991) Mutations affecting body organization in the *Arabidopsis* embryo. *Nature* **353**: 402–407
- McKenna A, Hanna M, Banks E, Sivachenko A, Cibulskis K, Kernytsky A, Garimella K, Altshuler D, Gabriel S, Daly M, et al** (2010) The genome analysis toolkit: A MapReduce framework for analyzing next-generation DNA sequencing data. *Genome Res* **20**: 1297–1303
- Meinke DW** (2019) Genome-wide identification of *<scp>EMBRYO</scp>* - *<scp>DEFECTIVE</scp>* (*<scp>EMB</scp>*) genes required for growth and development in *Arabidopsis*. *New Phytol* **nph.16071**
- Meinke DW** (2013) A survey of dominant mutations in *Arabidopsis thaliana*. *Trends Plant Sci* **18**: 84–91
- Meng F, Xiang D, Zhu J, Li Y, Mao C** (2019) Molecular Mechanisms of Root Development in Rice. *Rice*. doi: 10.1186/s12284-018-0262-x
- Moreno-Risueno MA, Van Norman JM, Moreno A, Zhang J, Ahnert SE, Benfey PN** (2010) Oscillating Gene Expression Determines Competence for Periodic *Arabidopsis* Root Branching. *Science* (80-) **329**: 1306–1311
- Mubarak S, Okabe Y, Fukuda N, Ariizumi T, Ezura H** (2015) Potential Use of a Weak Ethylene Receptor Mutant, *Sletr1-2*, as Breeding Material To Extend Fruit Shelf Life of Tomato. *J Agric Food Chem* **63**: 7995–8007
- Musseau C, Just D, Jorly J, Gévaudant F, Moing A, Chevalier C, Lemaire-Chamley M, Rothan C, Fernandez L** (2017) Identification of two new mechanisms that regulate fruit growth by cell expansion in tomato. *Front*

- Myouga F, Akiyama K, Tomonaga Y, Kato A, Sato Y, Kobayashi M, Nagata N, Sakurai T, Shinozaki K** (2013) The chloroplast function database II: A comprehensive collection of homozygous mutants and their phenotypic/genotypic traits for nuclear-encoded chloroplast proteins. *Plant Cell Physiol.* doi: 10.1093/pcp/pcs171
- Van Norman JM, Zhang J, Cazzonelli CI, Pogson BJ, Harrison PJ, Bugg TDH, Chan KX, Thompson AJ, Benfey PN** (2014) Periodic root branching in *Arabidopsis* requires synthesis of an uncharacterized carotenoid derivative. *Proc Natl Acad Sci U S A* **111**: E1300-9
- Oh K, Ivanchenko MG, White TJ, Lomax TL** (2006) The diageotropica gene of tomato encodes a cyclophilin: a novel player in auxin signaling. *Planta* **224**: 133–144
- Okabe Y, Ariizumi T, Ezura H** (2013) Updating the Micro-Tom TILLING platform. *Breed Sci* **63**: 42–48
- Persson S, Paredez A, Carroll A, Palsdottir H, Doblin M, Poindexter P, Khitrov N, Auer M, Somerville CR** (2007) Genetic evidence for three unique components in primary cell-wall cellulose synthase complexes in *Arabidopsis*. *Proc Natl Acad Sci U S A* **104**: 15566–15571
- Petit J, Bres C, Just D, Garcia V, Mauxion JP, Marion D, Bakan B, Joubès J, Domergue F, Rothan C** (2014) Analyses of tomato fruit brightness mutants uncover both cutin-deficient and cutin-abundant mutants and a new hypomorphic allele of GDSL Lipase. *Plant Physiol* **164**: 888–906
- Petricka JJ, Winter CM, Benfey PN** (2012) Control of *Arabidopsis* Root Development . *Annu Rev Plant Biol* **63**: 563–590
- Pysh L, Alexander N, Swatzyna L, Harbert R** (2012) Four alleles of AtCESA3 form an allelic series with respect to root phenotype in *Arabidopsis thaliana*. *Physiol Plant* **144**: 369–381
- Quinet M, Angosto T, Yuste-Lisbona FJ, Blanchard-Gros R, Bigot S, Martinez JP, Lutts S** (2019) Tomato Fruit Development and Metabolism. *Front Plant Sci.* doi: 10.3389/fpls.2019.01554
- Rick CM** (1991) Tomato paste: a concentrated review of genetic highlights from the beginnings to the advent of molecular genetics. *Genetics* **128**:
- Robbins NE, Dinneny JR** (2015) The divining root: Moisture-driven responses of roots at the micro- and macro-scale. *J Exp Bot* **66**: 2145–2154

- Rosquete MR, von Wangenheim D, Marhavý P, Barbez E, Stelzer EHK, Benková E, Maizel A, Kleine-Vehn J** (2013) An auxin transport mechanism restricts positive orthogravitropism in lateral roots. *Curr Biol* **23**: 817–22
- Rothan C, Bres C, Garcia V, Just D** (2016) Tomato Resources for Functional Genomics. pp 75–94
- Rothan C, Diouf I, Causse M** (2019) Trait discovery and editing in tomato. *Plant J* **97**: 73–90
- Saito T, Ariizumi T, Okabe Y, Asamizu E, Hiwasa-Tanase K, Fukuda N, Mizoguchi T, Yamazaki Y, Aoki K, Ezura H** (2011) TOMATOMA: A novel tomato mutant database distributing micro-tom mutant collections. *Plant Cell Physiol* **52**: 283–296
- Schneider CA, Rasband WS, Eliceiri KW** (2012) NIH Image to ImageJ: 25 years of image analysis. *Nat Methods* **9**: 671–675
- Scott J, Harbaugh B.** (1989) *Micro-Tom : A Miniature Dwarf Tomato*. Agricultural Experiment Station Institute of Food and Agricultural Sciences University of Florida, Gainesville FL
- Shikata M, Ezura H** (2016) *Micro-Tom Tomato as an Alternative Plant Model System: Mutant Collection and Efficient Transformation*. Humana Press, New York, NY, pp 47–55
- Shikata M, Hoshikawa K, Ariizumi T, Fukuda N, Yamazaki Y, Ezura H** (2016) TOMATOMA Update: Phenotypic and Metabolite Information in the Micro-Tom Mutant Resource. *Plant Cell Physiol* **57**: e11–e11
- Shirasawa K, Hirakawa H, Nunome T, Tabata S, Isobe S** (2016) Genome-wide survey of artificial mutations induced by ethyl methanesulfonate and gamma rays in tomato. *Plant Biotechnol J* **14**: 51–60
- Su S-H, Gibbs NM, Jancewicz AL, Masson PH** (2017) Molecular Mechanisms of Root Gravitropism. *Curr Biol* **27**: R964–R972
- Tateno M, Brabham C, DeBolt S** (2016) Cellulose Biosynthesis Inhibitors - A Multifunctional Toolbox. *J Exp Bot* **67**: 533–542
- Toal TW, Ron M, Gibson D, Kajala K, Splitt B, Johnson LS, Miller ND, Slovak R, Gaudinier A, Patel R, et al** (2018) Regulation of root angle and gravitropism. *G3 Genes, Genomes, Genet* **8**: 3841–3855
- Wachsman G, Modliszewski JL, Valdes M, Benfey PN** (2017) A simple pipeline for mapping point mutations. *Plant Physiol* **174**: 1307–1313

- Wang X, Xing Y** (2017) Evaluation of the effects of irrigation and fertilization on tomato fruit yield and quality: A principal component analysis. *Sci Rep*. doi: 10.1038/s41598-017-00373-8
- Wilson-Sánchez D, Rubio-Díaz S, Muñoz-Viana R, Pérez-Pérez JM, Jover-Gil S, Ponce MR, Micol JL** (2014) Leaf phenomics: a systematic reverse genetic screen for *Arabidopsis* leaf mutants. *Plant J*.
- Yu P, Baldauf JA, Lithio A, Marcon C, Nettleton D, Li C, Hochholdinger F** (2016) Root type-specific reprogramming of maize pericycle transcriptomes by local high nitrate results in disparate lateral root branching patterns. *Plant Physiol* **170**: 1783–1798
- Zheng H, Pan X, Deng Y, Wu H, Liu P, Li X** (2016) AtOPR3 specifically inhibits primary root growth in *Arabidopsis* under phosphate deficiency. *Sci Rep*. doi: 10.1038/srep24778
- Zhu F-Y, Chen M-X, Ye N-H, Qiao W-M, Gao B, Law W-K, Tian Y, Zhang D, Zhang D, Liu T-Y, et al** (2018) Comparative performance of the BGISEQ-500 and Illumina HiSeq4000 sequencing platforms for transcriptome analysis in plants. *Plant Methods* **14**: 69

Figures

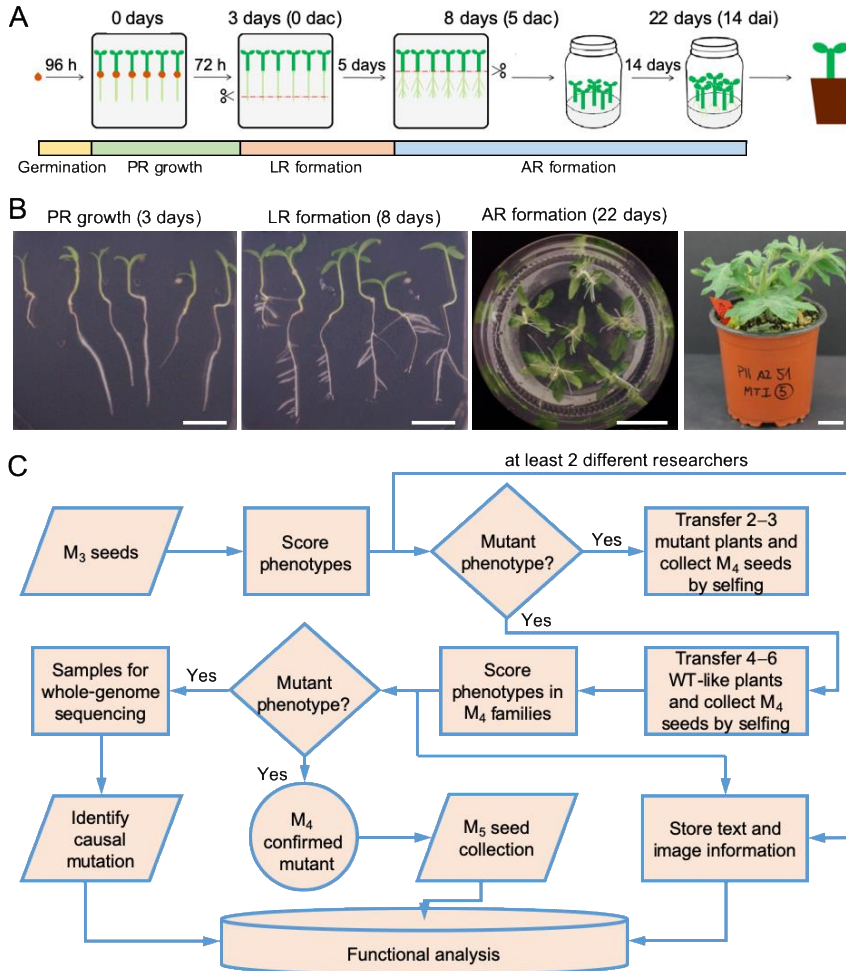


Figure 1. Design of the early seedling and RSA mutant screening in tomato. (A) Experimental layout used in this work. (B) Representative images of the studied phenological growth stages. Scale bars: 20 mm. (C) Workflow chart of our mutant screening. AR: adventitious root, dac: days after root tip cutting, dai: days after AR induction, LR: lateral root, PR: primary root, WT: wild type.

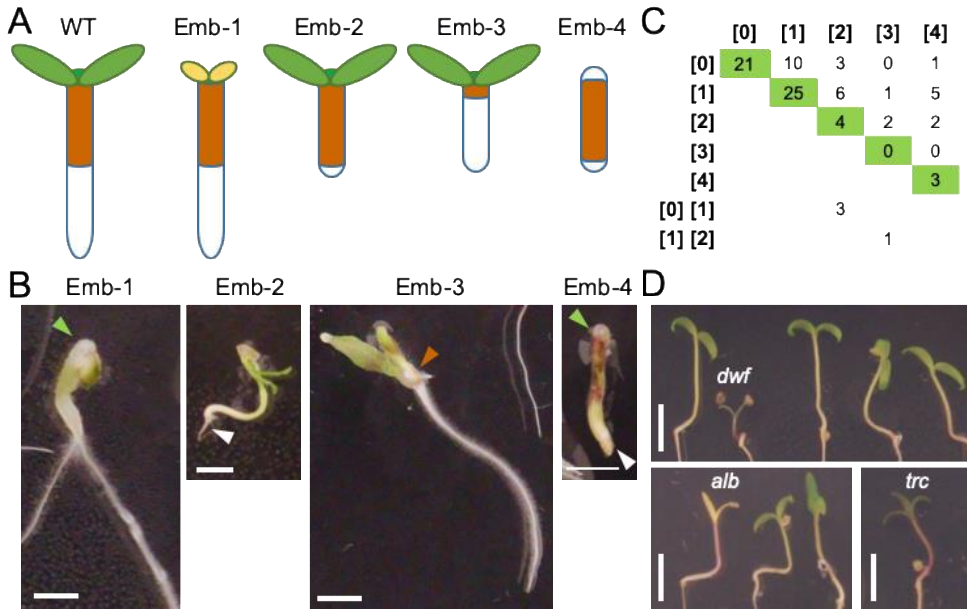


Figure 2. Tomato mutants with defective embryo development. (A) Schematic diagram of WT and Emb phenotypes found in our study. Emb-1 and Emb-2 mutants display apical or basal patterning defects, respectively. Emb-3 mutants lack the central domain of the embryo (i.e., the hypocotyl), while Emb-4 mutants resemble the *Arabidopsis gnom* mutants, with only the central domain present. (B) Representative images of the observed Emb phenotypes in tomato. Arrowheads indicate missing embryo structures (green: apical, brown: central, white: basal). (C) Number of M₃ lines segregating for the observed Emb phenotypes; [0] represents seedlings that stopped growth at stage 005 (Feller et al., 1995). (D) Representative images of some segregating shoot phenotypes, such as dwarf (*dwf*), albino (*alb*) or tricotyledon seedlings (*trc*). Scale bars: 5 mm.

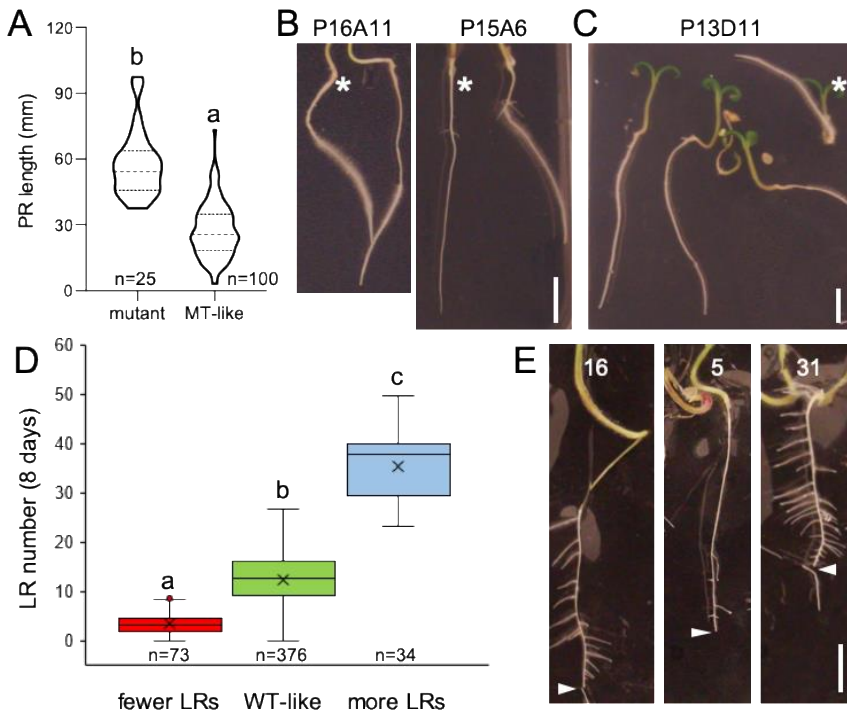


Figure 3. Rooting phenotypes studied during early growth in tomato. (A) Violin plot of PR lengths in putative mutants with increased values compared with those of their WT-like siblings. Dashed and dotted lines indicate median and quartiles, respectively. Letters indicate significant differences between groups (p -value <0.001). (B) Representative images of segregating root hair phenotypes (indicated by asterisks), such as an increased amount of root hairs in P16A11 and a decreased amount of root hairs in P15A6. (C) Agravitropic root phenotype segregating in the P13D11 line. (D) Boxplots of the LR number in putative mutants with decreased or increased values compared with those of their WT-like siblings. The average and median are shown. Letters indicate significant differences between groups (p -value <0.001). (E) Representative images of seedlings with average (left), reduced (middle) and increased (right) numbers of LRs. Scale bars: 10 mm.

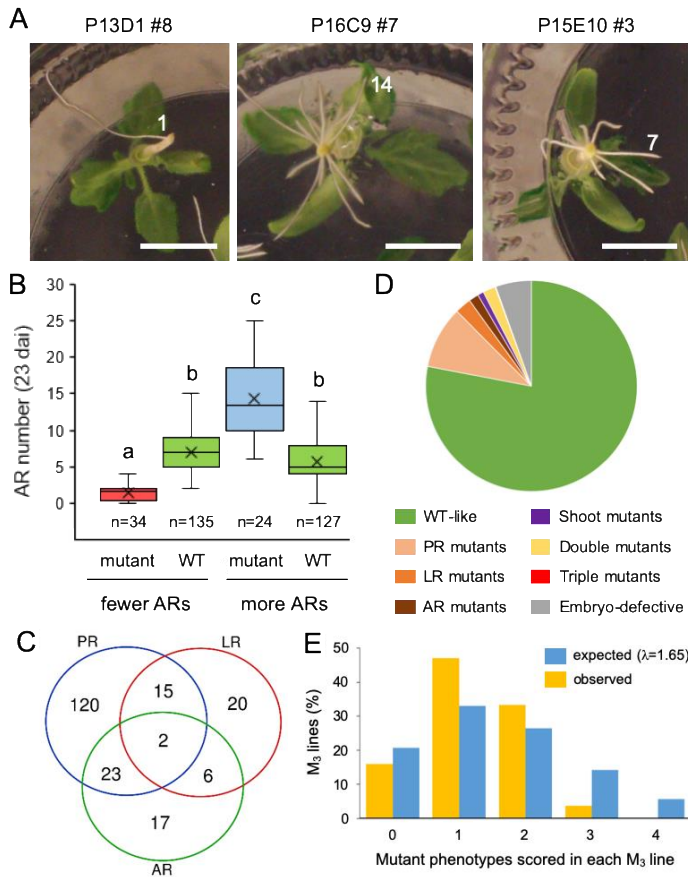


Figure 4. Wound-induced AR phenotypes. (A) Representative images of rooted hypocotyls of some mutants with reduced (P13D1 #8) or increased (P16C9 #7) AR numbers compared with the Micro-Tom background line (represented by P15E10 #3). Scale bar: 10 mm. (B) Boxplots of AR numbers in putative mutants with reduced or increased values compared with their WT-like siblings. The average and median are shown. Letters indicate significant differences between groups (p -value <0.001). (C) Venn diagram of the studied M₃ lines with annotated phenotypes for PR, LRs and ARs. (D) Percentage of early seedling and root mutant phenotypes studied. (E) Distribution of annotated mutations in the studied M₃ lines (orange) and Poisson distribution estimate for $\lambda=1.65$ (blue).

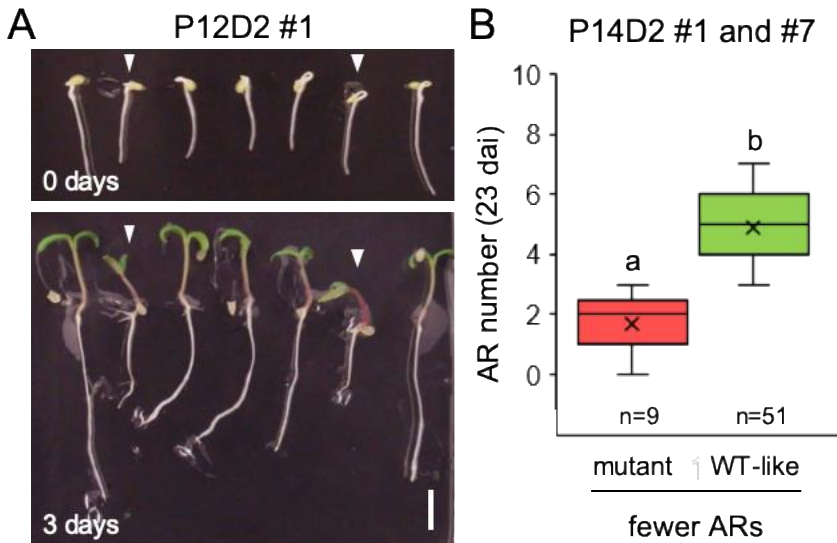


Figure 5. Genetic confirmation of early seedling and RSA tomato mutants. (A) Representative images of seedlings from an M₄ family segregating for plants with short-root and dwarf phenotypes; Scale bar: 10 mm. (B) Boxplots of AR numbers in two M₄ families from P14D2 segregating for mutants with decreased AR numbers. The average and median are shown. Letters indicate significant differences between groups (p-value<0.001).

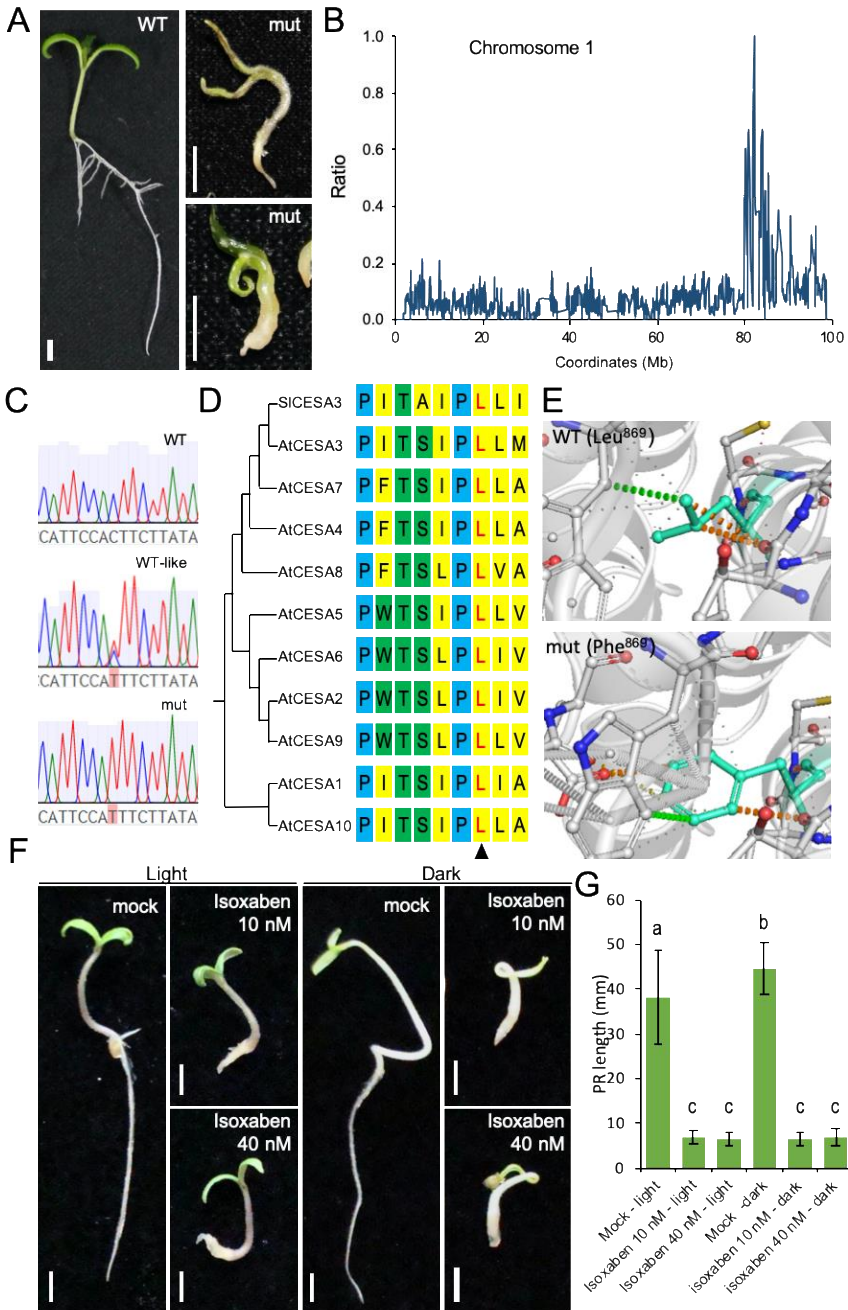


Figure 6. Molecular confirmation of early seedling and RSA tomato mutants. (A) Representative images of seedlings from the P14A1#2 M4 family segregating for plants with the studied seedling-lethal phenotype. Scale bars: 10 mm. (B) Genomic region of chromosome 1 associated with the studied mutant phenotype. The plot represents the allelic ratio for the studied SNPs along the chromosome using the average smoothing method. (C) Sanger electropherogram showing genotype-phenotype correlation for SNP candidate n°7. (D) Solyc01g087210 (SICESA3) and Arabidopsis CESA-family proteins (AtCESA) show strong amino acid conservation near the mutation site (black arrowhead). (E) Intramolecular interactions of Leu⁸⁶⁹ (WT) and Phe⁸⁶⁹ (mut) residues. Green and orange dashed lines represent hydrophobic contacts and hydrogen bonds, respectively; gray dashed lines represent aromatic interactions. (F) Representative images of isoxaben- and mock-treated seedlings under light (16/8) and dark conditions. (G) PR length of isoxaben- and mock-treated seedlings under light (16/8) and dark conditions. Scale bars: 50 mm.

Table 1. Early seedling and root mutant phenotypes studied.

Structure	Trait	Value	Description	Days
Germinated seedling	Development	Do not germinate	Radicle is not visible after 96 h at 28° C in darkness	0
		Delayed germination	A ≤4 mm radicle is visible after 96 h at 28° C in darkness	0
		Do germinate	A >4 mm radicle is visible after 96 h at 28° C in darkness	0
PR	Development	Absent	A functional PR is not observed in the seedling	3
		Present	A functional PR is observed in the seedling	3
		Embryonic lethality	Seedlings that were unable to complete organogenesis after germination	3
	Length	Decreased length	PR length is ≥25% lower from that of the average of the siblings	3
		Normal length	PR length is not different from that of the average of the siblings	3
		Increased length	PR length is ≥25% higher from that of the average of the siblings	3
	Gravitropism	Positive gravitropism	PR grows towards gravity vector	3
		Agravitropic	PR grows away gravity vector	3
		Root hair number	Decreased amount	Root hair number is ≥25% lower from that of the average of the siblings
	Normal amount		Root hair number is not different from that of the average of the siblings	3
	Increased amount		Root hair number is ≥25% higher from that of the average of the siblings	3
	LRs	Development	Absent	Functional LR is not observed within the PR
Present			Functional LR is observed within the PR	8
Number		Decreased amount	LR number is ≥25% lower from that of the average of the siblings	8

		Normal amount	LR number is not different from that of the average of the siblings	8
		Increased amount	LR number is $\geq 25\%$ higher from that of the average of the siblings	8
Shoot	Development	Dwarf	Shoot development is $\geq 25\%$ lower from that of the average of the siblings	8
		Delayed growth	Shoot development is delayed as regards that of the average of the siblings	8
		Normal size	Shoot development is not different from that of the average of the siblings	8
	Color	Albino	Absent shoot pigmentation due to lack of chlorophyll	8
	Cotyledons	Decreased amount	Cotyledons number is lower from that of the average of the siblings	8
		Normal amount	Cotyledons number is not different from that of the average of the siblings	8
Increased amount		Cotyledons number is higher from that of the average of the siblings	8	
ARs	Development	Absent	Functional ARs are not observed at the lower hypocotyl	23
		Present	Functional ARs are observed at the lower hypocotyl	23
	Number	Decreased amount	AR number is $\geq 25\%$ lower from that of the average of the siblings	23
		Normal amount	AR number is not different from that of the average of the siblings	23
		Increased amount	AR number is $\geq 25\%$ higher from that of the average of the siblings	23

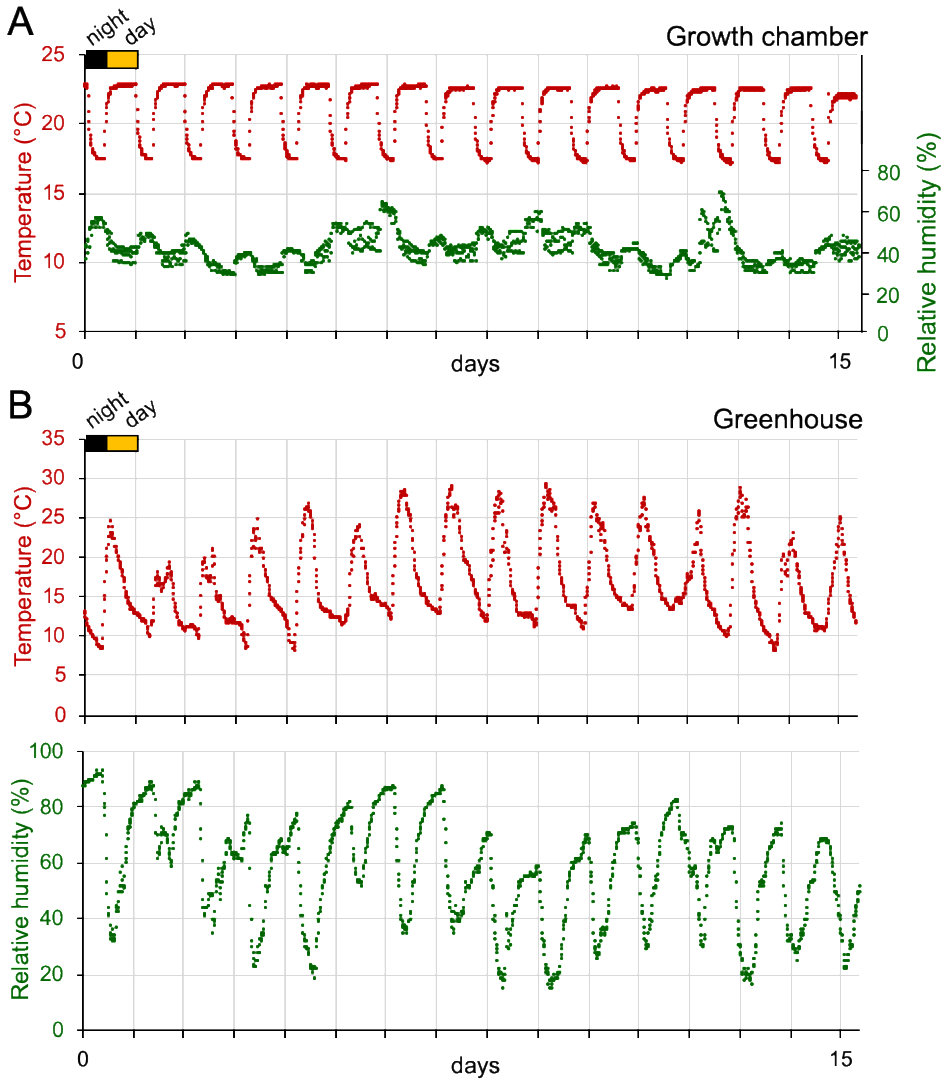
Table 2. Confirmation of early root mutants in M4 families.

M₃ line	M₃ mutant phenotypes (<i>m1</i>; <i>m2</i>)	M₄ family	WT	<i>m1</i>	<i>m2</i>	<i>m1m2</i>	χ^2 (segregation); hypothesis¹
P11H4	shorter PR; seedling lethal	P1#2 WT-like	14				4.667 (3:1)
		P1#3 WT-like	13	4	2		2.146 (9:3:4); recessive epistasis (<i>m2</i> > <i>m1</i>)
		P2#3 <i>m1</i>		14		4	0.074 (3:1); <i>m1</i> homozygous, segregates for <i>m2</i>
P11H8	shorter PR	P2#3 WT-like	15	2			1.588 (3:1); segregates for a recessive mutation (<i>m1</i>)
		P2#6 WT-like	17	2			2.123 (3:1); segregates for a recessive mutation (<i>m1</i>)
		P2#8 WT-like	16				5.333 (3:1)
P12A1	shorter PR	P1#3 WT-like	18	3			1.286 (3:1); segregates for a recessive mutation (<i>m1</i>)
		P1#7 MT-like	18				6.000 (3:1)
P12A6	shorter PR	P1#1 WT-like	19				6.333 (3:1)
		P1#2 WT-like	10	7			2.373 (3:1); segregates for a recessive mutation (<i>m1</i>)
P12A7	shorter PR	P1#1 WT-like	19				6.333 (3:1)
		P1#2 WT-like	20				6.667 (3:1)
		P1#3 WT-like	19				6.333 (3:1)
P12C12	shorter PR	P1#7 WT-like	15	5			0.000 (3:1); segregates for a recessive mutation (<i>m1</i>)
		P1#8 WT-like	14	3			0.490 (3:1); segregates for a recessive mutation (<i>m1</i>)
P12D2	shorter PR	P1#1 WT-like	13	3			0.333 (3:1); segregates for a recessive mutation (<i>m1</i>)
		P1#3 WT-like	14				4.667 (3:1)
		P2#1 WT-like	17	4			0.397 (3:1); segregates for a recessive mutation (<i>m1</i>)
P12G2	shorter PR	#3 WT-like	14	8			1.515 (3:1); 0.488 (9:7); dominant epistasis
		#5 WT-like	13	9			2.970 (3:1); 0.072 (9:7)
		#6 WT-like	16	8			0.889 (3:1); 1.058 (9:7)
P14A1	shorter PR; seedling lethal	#2 WT-like	17	3	4		2.074 (9:3:4); recessive epistasis (<i>m2</i> > <i>m1</i>)
		#15 WT-like	21	3			2.000 (3:1); segregates for a recessive mutation (<i>m1</i>)
P14A9	shorter PR; seedling lethal	#1 WT-like	21	3	5		3.138 (9:3:4); recessive epistasis (<i>m2</i> > <i>m1</i>)
		#9 WT-like	24				8.000 (3:1)
P14A12	shorter PR; seedling lethal	#3 WT-like	21	3			2.000 (3:1); segregates for a recessive mutation (<i>m1</i>)
		#4 WT-like	22				7.333 (3:1)
P14B4	shorter PR; seedling lethal	#7 WT-like	12	2			0.857 (3:1); segregates for a recessive mutation (<i>m1</i>)
		#1 WT-like	17	5			0.061 (3:1); segregates for a recessive mutation (<i>m1</i>)

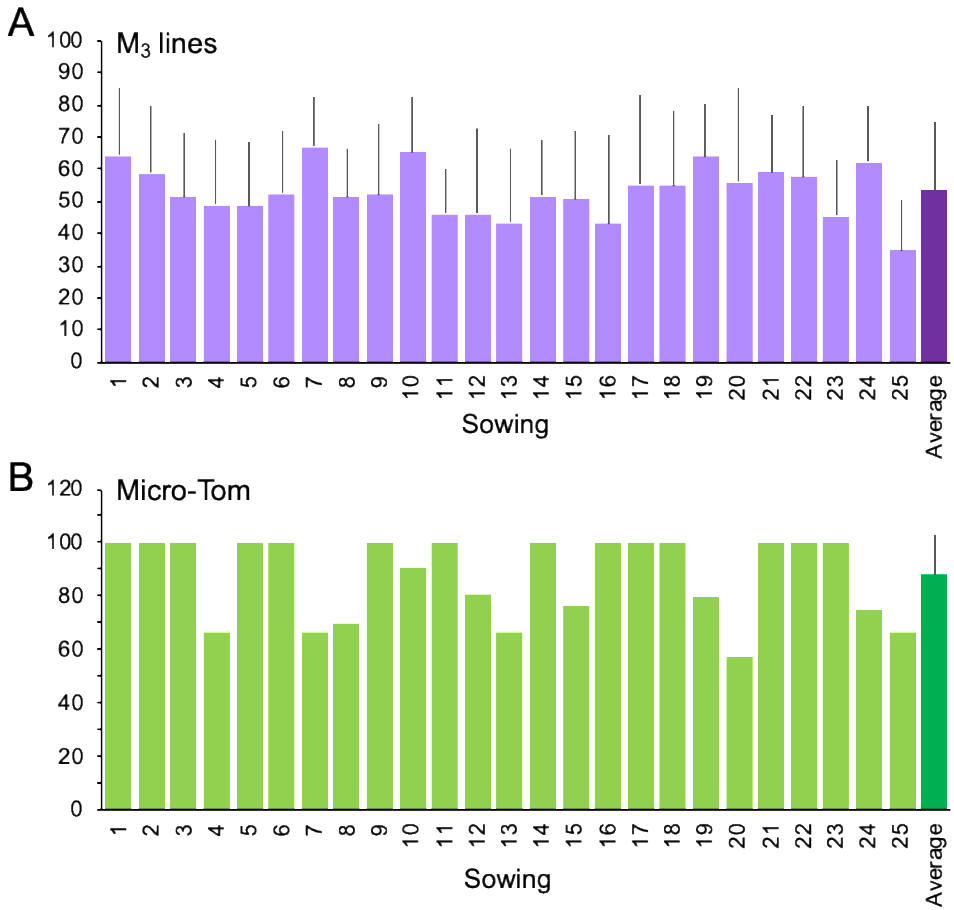
		#2 WT-like	20	3	4	3.486 (9:3:4); recessive epistasis ($m2>m1$)
		#3 WT-like	19	6		0.013 (3:1); segregates for a recessive mutation ($m1$)
P14C12	shorter PR; seedling lethal	#4 WT-like	14	7	8	0.854 (9:3:4); recessive epistasis ($m2>m1$)
		#5 WT-like	26	4		2.178 (3:1); segregates for a recessive mutation ($m1$)
P14D2	decreased AR number; seedling lethal	#1 WT-like	25	4		1.943 (3:1); segregates for a recessive mutation ($m1$)
		#7 WT-like	25	5		1.111 (3:1); segregates for a recessive mutation ($m1$)
		#4 WT-like	17	3	4	1.463 (9:3:3:1); two unlinked recessive mutations
P14D10	shorter PR; decreased LR number	#6 WT-like	13		5	0.074 (3:1); segregates for a recessive mutation ($m2$)
		#8 WT-like	19	5		0.222 (3:1); segregates for a recessive mutation ($m1$)
		#2 WT-like	15	7	8	0.578 (9:3:4); recessive epistasis ($m2>m1$)
P16F4	longer PR; seedling lethal	#4 WT-like	26	4		1.943 (3:1); segregates for a recessive mutation ($m1$)
		#5 WT-like	23	4	3	5.393 (9:3:4); recessive epistasis ($m2>m1$)

¹ The χ^2 values in italics indicate that the observed data do not fit the expected segregation of the mutant phenotype to the proposed hypothesis (p -value<0.05).

Supplementary figures and tables



Supplementary Figure S1. Air temperature and relative humidity during the phenotype screening. (A) Growth chamber conditions. (B) Greenhouse conditions. A representative 15-days window is shown. Data points were taken every 15 min.



Supplementary Figure S2. Germination percentage for the studied lines. (A) M₃ lines. (B) Micro-Tom background used as a reference.

Supplementary Table S1. Tomato EMS lines studied in this work.

Sowing	Identification code¹	n
01	P11G6, P11G7, P11G8, P11G9, P11G10, P11G11, P11G12, P11H1, P11H2, P11H3, P11H4, P11H5, P11H6, P11H7, P11H8, P11H9, P11H10 , P11H11, P11H12	1
02	P12A1, P12A2, P12A3 , P12A4, P12A5, P12A6, P12A7, P12A8, P12A9, P12A10, P12A11, P12A12, P12B1, P12B2, P12B3 , P12B4, P12B5 , P12B6, P12B7, P12B8	2
03	P12B9, P12B10, P12B11, P12B12, P12C1 , P12C2, P12C3, P12C4, P12C5, P12C6, P12C7, P12C8, P12C9 , P12C10, P12C11, P12C12, P12D1 , P12D2, P12D3 , P12D4	2
04	P13C12, P13D1, P13D2, P13D3 , P13D4 , P13D5, P13D6, P13D9, P13D10 , P13D11, P13D12 , P12E1, P12E2, P12E3 , P12E4 , P12E5, P12E6 , P12E7, P12E8, P12E9	2
05	P12E10 , P12E11 , P12E12, P12F1, P12F2 , P12F3, P12F4, P12F5 , P12F6, P12F7 , P12F8 , P12F9, P12F10, P12F11 , P12F12, P12H1 , P12H2 , P12H3, P12H4, P12H5	2
06	P12H6, P12H7, P12H8, P12H9 , P12H10 , P12H11, P12H12, P12G1, P12G2, P12G3 , P12G4, P12G6 , P12G7, P12G8, P12G9, P12G10 , P12G11, P12G12	1
07	P14A1, P14A2, P14A3, P14A4 , P14A5, P14A6, P14A7, P14A8, P14A9, P14A10, P14A11, P14A12, P14B1, P14B2, P14B3, P14B4	1
08	P14B5, P14B6 , P14B7, P14B8 , P14B10, P14B11, P14B12, P14C1, P14C2, P14C3, P14C4, P14C5, P14C6, P14C7, P14C8, P14C9	1
09	P14C10, P14C11, P14C12, P14D1 , P14D2, P14D3 , P14D4, P14D5, P14D6, P14D7, P14D8, P14D9, P14D10, P14D11	1
10	P14D12, P14E1, P14E2, P14E3, P14E4, P14E5, P14E6, P14E7, P14E8, P14E9, P14E10, P14E12, P14F1, P14F2, P14F3, P14F4, P14F5	1
11	P14F6, P14F7, P14F8, P14F9, P14F10, P14F11, P14F12, P14G1, P14G2, P14G3, P14G4, P14G5 , P14G6, P14G8, P14G9 , P14G10, P14G11	1
12	P14G12, P14H1, P14H2 , P14H3 , P14H4, P14H5, P14H6 , P14H7, P14H8, P14H9, P14H10, P14H11, P14H12 , P15A1, P15A2 , P15A3, P14A4	1
13	P15A10, P15A11, P15A12 , P15B1 , P15B2 , P15B3, P15B4, P15B5, P15B6 , P15B7, P15B8, P15B9, P15B10, P15B11	1
14	P15B12, P15C1, P15C2 , P15C3 , P15C4 , P15C5, P15C6 , P15C7, P15C8, P15C9, P15C10, P15C11, P15C12, P15D1	1
15	P15D2, P15D3, P15D4 , P15D5 , P15D6, P15D7, P15D8, P15D9, P15D10 , P15D11 , P15D12, P15E1, P15E2, P15E3	1
16	P15E4, P15E6 , P15E7, P15E8 , P15E9 , P15E10, P15E11, P15E12, P15F1 , P15F2, P15F3, P15F4 , P15F5 , P15F6	1
17	P15F7, P15F8, P15F9, P15F10 , P15F11 , P15F12, P15G1, P15G2, P15G3, P15G4, P15G5, P15G6, P15G7 , P15G8	1
18	P15G9, P15G10, P15G11 , P15G12, P15H1 , P15H2, P15H3, P15H4 , P15H5 , P15H6, P15H7, P15H8, P15H9, P15H10	1
19	P15H11 , P16A1, P16A2, P16A3 , P16A5, P16A6, P16A7 , P16A8, P16A9, P16A10, P16A11, P16A12, P16B1, P16B3	1
20	P16B4, P16B5 , P16B6, P16B7, P16B8, P16B9, P16B10, P16B11, P16B12 , P16C1 , P16C2 , P16C3 , P16C4, P16C5	1

21	P16C6, P16C7, P16C8, P16C9, P16C10 , P16C11, P16C12, P16D1, P16D2 , P16D3, P16D4, P16D5, P16D6, P16D7	1
22	P16D8, P16D9, P16D10 , P16D11, P16D12 , P16E1, P16E2 , P16E3 , P16E4, P16E5, P16E6, P16E7 , P16E8, P16E9	1
23	P16E10, P16E11, P16E12, P16F1 , P16F2 , P16F3, P16F4, P16F7, P16F8 , P16F9, P16F10 , P16F11 , P16F12, P16G1	1
24	P16G3, P16G4, P16G5, P16G6, P16G7, P16G8, P16G9, P16G10, P16G11 , P16G12 , P16H1, P16H2, P16H3, P16H4	1
25	P15A5, P15A6, P15A7, P15A8, P15A9, P16H5 , P16H6 , P16H7, P16H8, P16H9 , P16H10, P16H11, P16H12	1

¹M₃ lines with less than eight germinated seedlings (in bold) were not further studied (n = 95).